IEEE Access
Multidisciplinary ⋮ Rapid Review ⋮ Open Access Journal

Received April 15, 2018, accepted May 17, 2018, date of publication May 22, 2018, date of current version June 19, 2018.

Digital Object Identifier 10.1109/ACCESS.2018.2839679

Research Into a Recovery Method of GNSS Authorized Service Signal Component

WEI XIAO, WENXIANG LIU, WEIHUA MOU, LING YONG, AND GUANGFU SUN
College of Electronic Science, National University of Defense Technology, Changsha 410073, China

Corresponding author: Guangfu Sun (gfsun@163.com)

This work was supported by NSFC under Project 41604016.

ABSTRACT A code recovery method of a global navigation satellite system (GNSS) authorized service (AS) signal component is described under the condition of a high signal-to-noise ratio. The correctness of the spreading code verification can be used to monitor the health status of satellite payloads. Pseudo code recovery is a precondition to verify the validity of pseudo code. For a specified GNSS signal multiplexing approach, the distribution of baseband signal phase points on a constellation diagram is established. The open service signal component and the AS signal component correlate with each other on the unit circle. By wiping off the signal carrier, each signal component can be recovered according to the phase table of the transmitted signal. Different states of the global positioning system L1 signal is introduced, and the AS signal component recovery performance under different constant enveloping modulations is analyzed. This paper provides a reference for the analysis, evaluation, and system optimization design of a GNSS signal. Relevant research results can be applied to satellite signal quality monitoring and electronic reconnaissance.

INDEX TERMS GPS modernization, code sequence recovery, authorized service signal, bit error rate.

I. INTRODUCTION

Bit error rate (BER) is always used to measure the performance of demodulation and decoding after carrier tracking. The verification of spreading code symbol correctness can be used to monitor the health status of a satellite payload, which is an important part of navigation signal monitoring and evaluation [1]. The spreading pseudo code sequence recovery is the basis of analyzing the BER. Many spreading code symbol errors occur in a short time when the satellite payload fails. Therefore, we can distinguish a code error produced either by a satellite failure or by noise via the BER. In general, for continuous code error analysis, a bit error rate over 1×10^{-3} may be considered a fault caused by a satellite payload failure [2].

The past 20 years have witnessed tremendous developments of new and modernized satellite-based navigation systems, including Global Navigation Satellite Systems (GNSSs), regional systems, and space-based augmentation systems (SBASs). Fig. 1 shows the evolution of the GPS signals over satellite blocks [3]. The legacy Global Positioning System (GPS) signals include the coarse/acquisition (C/A) code and the precision code signal on radio frequency (RF) link 1 (L1) carrier frequency of 1575.42 MHz [4]. The C/A code is open (unencrypted) and the P code signal is only intended for authorized (military) use and is normally encrypted (referred to as the P(Y) code). Both legacy GPS signals are generated using direct sequence spread spectrum (DSSS) modulation. A new long pseudo-noise (PN) sequences code called M-code has been proposed and transmitted by the Block IIF SVs. Advanced encryption algorithms guarantee M-code sequence a much higher confidentiality than P(Y) code [5]. The new civil signal called L1C which will be broadcast on the L1 carrier frequency is an intergral part of the GPS III capabilities being developed. The new signal consists of two main components; one denoted $L1C_P$ to represent a pilot signal, without any data message, and $L1C_D$ that is spread by a ranging code and modulated by a data message [6].

Civilian GNSS services have open codes and signal structure, which make it feasible that anybody with adequate knowledge can reproduce the legitimate signals in an exact manner [7]. A high-gain antenna is always used to receive and analyze the navigation signal in signal monitoring and evaluation systems [8]. For the legacy GPS L1 signal, C/A and P(Y) codes at L1 are on the same carrier, but placed 90° apart and these two are summed together to produce the L1 signal.

The C/A codes can be recovered by tracking the received signal. In addition, the symbol polarity of the P(Y) signal component can be judged by the orthogonal relationship

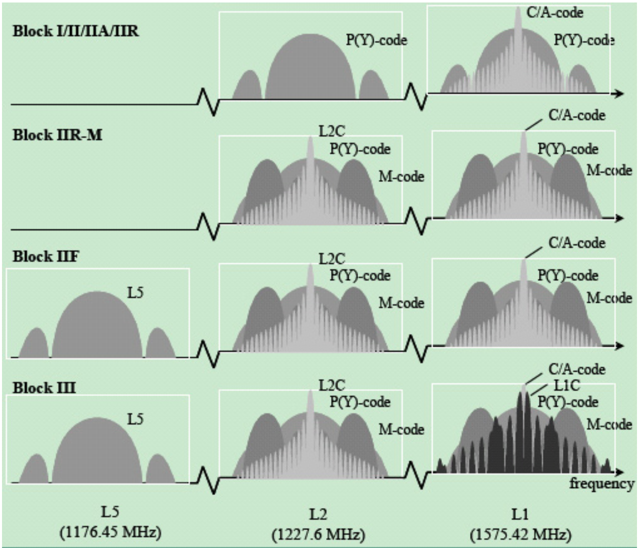

FIGURE 1. Evolution of the GPS Signals.

TABLE 1. Available signals transmitted by different GPS satellite blocks on l1 carrier.

GPS Blocks	Signal component	Modulation	Service
Block I/II/IIA/IIR	L1 C/A	BPSK(1)	OS
	L1 P(Y)	BPSK(10)	AS
Block IIR/IIF	L1 C/A	BPSK(1)	OS
	L1 P(Y)	BPSK(10)	AS
	L1 M	BOCc(10,5)	AS
Block III	L1 C/A	BPSK(1)	OS
	L1 P(Y)	BPSK(10)	AS
	L1 M	BOCc(10,5)	AS
	L1 C_D	BOC(1,1)	OS
	L1 C_P	TMBOC(6,1)	OS

between the Open Service (OS) and Authorized Service (AS) signal branches. However, a modern GNSS widely transmits multiple signals to provide different levels of services. Since the payload power of a satellite is limited, multiple signals must be combined into a composite signal and transmitted by a single source [9]. Various channel signals form a more complex phase relationship with each other, making it difficult to differentiate signal components through the inphase/quadrature (I/Q) branches after carrier tracking. The available signals transmitted by different GPS blocks on L1 band are summarized in Table 1 [10]. The M-code uses a variant of DSSS modulation referred to as binary offset carrier (BOC). L1C uses a mixture of two BOC modulations referred to as multiplexed BOC (MBOC). The L1C_D signal is modulated on the L1 RF carrier using a BOC (1,1) modulation technique. The L1C_P signal is modulated on the L1 RF carrier using a Time-Multiplexed BOC (TMBOC) modulation technique. The TMBOC technique utilized by L1C_P signal uses a combination of BOC (1,1) and BOC (6,1) modulation [6].

For a baseband signal after a carrier wiped off, this paper analyses the Carrier to Noise Ratio (CNR) required to correctively recover the specific AS signal code combination. The code combination may be the Pseudo Random Noise (PRN) code, modulated with either navigation data or a secondary code, or both.

In the end, this paper takes the GPS L1 signal for example, and analyses the demodulation BER of the AS signal component under different CNRs, providing a reference for the analysis, evaluation and system optimization design of the GNSS signal. The research can be applied to the satellite signal quality monitoring and electronic surveillance.

II. DUAL-CHANNEL SIGNAL DEMODULATION THRESHOLD

Dual-channel navigation signals usually adopt an orthogonal multiplexing method. The dual-channel spreading codes modulate on two mutual orthogonal carriers, without disturbing each other, and the multiplexing efficiency reaches 100%. The baseband expression of the dual-channel signal adopted orthogonal multiplexing and can be expressed as:

$$S(t) = \sqrt{P_I} s_I + j\sqrt{P_Q} s_Q \tag{1}$$

where P_I and P_Q are the total powers of the in-phase and quadrature signal components, j is the imaginary unit. The in-phase and quadrature components of the carrier are given by $s_{I/Q}(t) = D_{I/Q}(t) \cdot C_{I/Q}(t)$, where $C(t)$ is the PRN spreading code, and $D(t)$ is the Navigation Data modulation. The secondary code and BOC modulation are easy to achieve in the next steps based on different code period and code frequency [1].

For the navigation signal containing only dual-channel signal components using binary level symbols, there are four kinds of combinations corresponding to four phase states. If orthogonal multiplexing is adopted, the dual-channel signal can be separated into two channels according to the orthogonal relationship, and each channel can be regarded as a Binary Phase Shift Keying (BPSK) modulation.

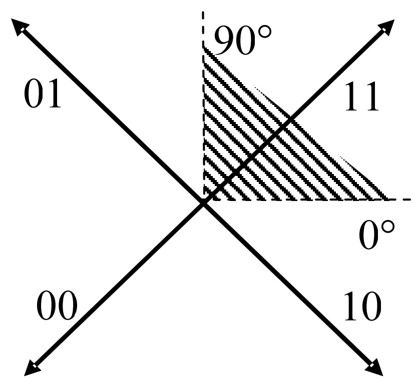

FIGURE 2. QPSK noise tolerance.

As shown in Fig. 2, for a Quadrature Phase Shift Keying (QPSK) modulation signal, the phase deviation of the signal vector caused by the noise will lead to a wrong judgement. For example, the transmitted signal phase of 45°

represents the baseband signal element "11". If it is affected by noise, the phase of the received vector may turn into 135°, and thus, it is misjudged as "01". When different outbound vectors transmit in equal probability, a rational decision threshold should be set at the position that is equidistance between the adjacent vector and the other vector. For the case of the vector "11" in Fig. 2, the threshold should be set at 0° and 90°. If the transmitted symbol is "11", error justice will occur when the phase of the received signal vector is beyond this range (shaded area).

Therefore, for the dual-channel navigation signals, if the signal symbol is judged by the polarity of the I/Q branch, the bit error rate performance is approximately equal to the average bit error rate of the BPSK signal [11].

$$P_e = Q\left(\sqrt{r}\right) \quad (2)$$

where r represents signal to noise ratio (SNR), Q is the normal right tail function (Q- function).

We take the legacy L1 signal as an example, that is, the C/A code is modulated on the in-phase channel whereas the P(Y) code is modulated on the quadrature phase channel, with both power ratios fulfilling the requirements of the Interface Control Document (ICD). The C/A code sequence is known by tracking the C/A signal. Then, the signal polarity is decoded to recover the chip symbol.

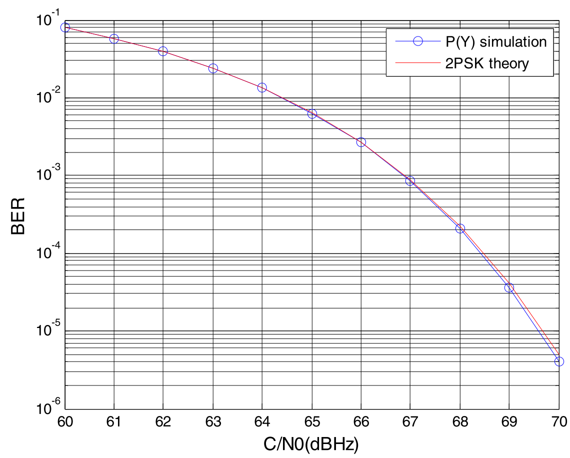

FIGURE 3. P(Y) code error rate for dual-channel signal case.

BER results are shown in Fig. 3 by comparing the recovered code with the original code sequence. As shown in Fig. 3, the lateral axis indicates the total C/N_0 of the compound signal, the red line represents the theoretical bit error rate of the BPSK signal, and the blue line represents the recovery P(Y) bit error rate. It can be seen that the recovery BER in a dual-channel signal orthogonal multiplexing is similar to the BPSK BER performance. Within the BER requirements of 10^{-3}, the AS signals can be fully recovered when the C/N_0 is greater than 67 dBHz. For lower BER requirements, greater C/N_0 is needed for signal monitoring.

It should be noted that as the probability of each transmitted navigation signal is not exactly equal, and the power level of the GPS L1 C/A code signal is different from that of the P(Y) code signal, the BER performance of P(Y) should be a little larger.

III. TRI-CHANNEL SIGNAL DEMODULATION THRESHOLD

In addition to the constant-envelope modulation (CEM) methods such as QPSK, Tri-Channel Signal multiplexing techniques are required for some special cases, such as the E1 band for Galileo and the L1 band for GPS Block IIRM and Block IIF. By employing these CEM methods, several signals can be combined into a constant-envelope composite signal and be transmitted through a single transmitter. Until now, several constant-envelope multiplexing methods have been proposed for tri-channel signal demodulation, such as Majority Voting (MV) [12], Interplex [13] and Coherent Adaptive Subcarrier Modulation (CASM) [14], with Interplex mathematically equivalent to CASM. Therefore, this paper takes Interplex multiplexing technology as an example. The baseband signal of Interplex modulation after normalization can be represented as

$$S(t) = I(t) + jQ(t) \quad (3)$$

where the in-phase and quadrature signals, I(t) and Q(t), are given by

$$\begin{aligned} I(t) &= \sin\theta_2 \cos\theta_3 \cdot s_2 + \cos\theta_2 \sin\theta_3 \cdot s_3 \\ Q(t) &= -\cos\theta_2 \cos\theta_3 \cdot s_1 + \sin\theta_2 \sin\theta_3 \cdot s_1 s_2 s_3 \end{aligned} \quad (4)$$

s_1, s_2, and s_3 represent the tri-channel signals adopted the Interplex multiplexing method. θ_2 and θ_3 are modulation angles, where $\theta_2, \theta_3 \neq k\pi/2$.

TABLE 2. The Relationship between the transmitted signal component and I/Q branch signal.

$s_1(t)$	$s_2(t)$	$s_3(t)$	In-phase signal	Quadrature phase signal
1	1	1	$\sin(\theta_2+\theta_3)$	$-\cos(\theta_2+\theta_3)$
1	1	-1	$\sin(\theta_2-\theta_3)$	$-\cos(\theta_2-\theta_3)$
1	-1	1	$-\sin(\theta_2-\theta_3)$	$-\cos(\theta_2-\theta_3)$
1	-1	-1	$-\sin(\theta_2+\theta_3)$	$-\cos(\theta_2+\theta_3)$
-1	1	1	$\sin(\theta_2+\theta_3)$	$\cos(\theta_2+\theta_3)$
-1	1	-1	$\sin(\theta_2-\theta_3)$	$\cos(\theta_2-\theta_3)$
-1	-1	1	$-\sin(\theta_2-\theta_3)$	$\cos(\theta_2-\theta_3)$
-1	-1	-1	$-\sin(\theta_2+\theta_3)$	$\cos(\theta_2+\theta_3)$

In general, for navigation signals containing tri-channel signal components, there are eight kinds of pseudo code combinations, namely, a maximum of eight phase states. The carrier phase of the transmitted signal at any time is determined by the combination of the code sequence. The relationship between the transmitted signal component and I/Q channel signal is shown in Table 2.

The scatterplot of the baseband signals is shown in Fig. 4, which contains tri-channel signal components adopting the

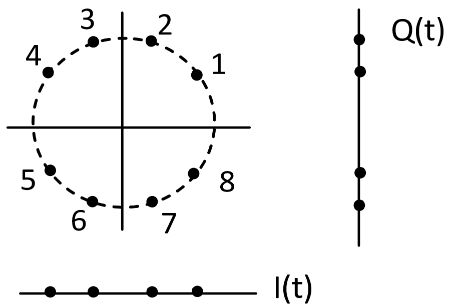

FIGURE 4. Scatterplot of tri-channel signal interplex modulation.

Interplex modulation. Assuming the first phase point to be $(x_1, y_1) = (\sin(\theta_2 + \theta_3), \cos(\theta_2 + \theta_3))$, then there are two possibilities for the second phase point based on the phase relationship of $(x_1, y_1) = (\sin(\theta_2 - \theta_3), \cos(\theta_2 - \theta_3))$ and θ_3. We first consider that $(x_2, y_2) = (\sin(\theta_2 - \theta_3), \cos(\theta_2 - \theta_3))$.

From the normalized signal phase constellation, the distance between the first two points can be expressed as $d_{12} = 2\sin\theta_3$, and the distance between the first phase point and the eight phase point can be defined as $d_{18} = 2\cos(\theta_2 + \theta_3)$. Because the first phase point error is only derived from the second phase point and the eighth phase point in a binary decision, then the bit error rate is

$$\begin{aligned} P_e(1,2) &= \mathrm{Q}\left(\frac{d_{12}}{2\sigma}\right) = \mathrm{Q}\left(\sqrt{2r}\sin\theta_3\right) \\ P_e(1,8) &= \mathrm{Q}\left(\frac{d_{18}}{2\sigma}\right) = \mathrm{Q}\left(\sqrt{2r}\cos\left(\theta_2 + \theta_3\right)\right) \end{aligned} \tag{5}$$

where Q(x) is the normal cumulative distribution function. The first phase point error can be determined by

$$P_{e,1} = P_e(1,2) + (1 - P_e(1,2))\, P_e(1,8) \tag{6}$$

The second phase point error can be obtained by the same method. There are three kinds of minimum distances between each phase point through all the possible phase states.

$$\begin{aligned} d_1 &= |2\sin\theta_k| \quad \text{or} \quad |2\cos\theta_k|\,(k = 2 \text{ or } 3) \\ d_2 &= |\cos(\theta_2 + \theta_3)|\,, d_3 = |\sin(\theta_2 - \theta_3)| \end{aligned} \tag{7}$$

Thus, the total bit error rate of the system can be expressed as

$$P_e \approx \mathrm{Q}(\frac{\sqrt{2r}}{2}d_1) + \frac{1}{2}\left(\mathrm{Q}\left(\frac{\sqrt{2r}}{2}d_2\right) + \mathrm{Q}\left(\frac{\sqrt{2r}}{2}d_3\right)\right) \tag{8}$$

When the 8 phase points are uniformly distributed in a unit circle, the constellation diagram is equivalent to that of the 8PSK, and the BER is the smallest.

$$P_e \approx 2\mathrm{Q}\left(\sqrt{2r}\sin\frac{\pi}{8}\right) \tag{9}$$

A set of possible solutions is $\theta_2 = \pi/4$ and $\theta_3 = \pi/8$.

Therefore, for the three navigation signals using the Interplex multiplexing method, the best code recovery performance is no more than 8PSK.

It should be noted that the constellation diagram may contain only six phase states under special circumstances such as $\theta_2 \pm \theta_3 = k\pi$. Then, there are two or more phases that correspond to the same phase point. It is difficult to recover the corresponding signal based only on the constellation phase point, if we know nothing about the three signals.

A. TWO CHANNELS UNKNOWN

If there is only one channel signal known for a tri-channel signal adopted Interplex multiplexing method. The OS code can be acquired after tracking the received baseband signal, which can be helpful to recover the AS signal components.

The $s_1(t)$, $s_3(t)$ in (4) can be recovered if the $s_2(t)$ is known in an ideal condition without noise.

$$\begin{aligned} r_{s3}(t) &= sign\left[\frac{I(t) - s_2(t)\cdot\sin\theta_2\cos\theta_3}{\cos\theta_2\sin\theta_3}\right] \\ r_{s1}(t) &= sign\left[\frac{Q(t)\cdot\cos\theta_2}{I(t)\cdot s_2(t)\cdot\sin\theta_2 - \cos\theta_3}\right] \end{aligned} \tag{10}$$

The noise items of the I/Q branch is considered, which are independent of each other. Iterate through all the launch phase combinations, and the recovered signal component $s_3(t)$ can be expressed as $r_{s3}(t) = sign\left[s_3(t) + \frac{n_I(t)}{\cos\theta_2\sin\theta_3}\right]$. In other words, the BER of $s_3(t)$ may be rewritten as

$$P_3 = Q\left(\sqrt{r}\,|\cos\theta_2\sin\theta_3|\right) \tag{11}$$

At the same time, if the $s_3(t)$ is known, the BER of $s_2(t)$ becomes

$$P_2 = Q\left(\sqrt{r}\,|\sin\theta_2\cos\theta_3|\right) \tag{12}$$

If the $s_1(t)$ is known, which is only found in quadrature channel, the $s_2(t)$ and $s_3(t)$ become more difficult to recover in the in-phase channel. In other words, their BER is greater than the condition of a known in-phase channel signal.

In summary, for the three signals adopted Interplex multiplexing method, in-phase channel code recovery performance can be evaluated as (11) and (12) when the other signal component in in-phase channel is known.

B. ONE CHANNEL UNKNOWN

If two channel signals are OS signals in a tri-channel signal adopted Interplex multiplexing method, the residual AS signal can be recovered with the help of tracking the two OS signals. For example, the $s_2(t)$ and $s_3(t)$ are known in (4). As the $s_1(t)$ is only in quadrature channel, the recovered $s_1(t)$ in the condition without noise can be expressed as

$$r_{s1}(t) = sign\left[\frac{-Q(t)}{\cos(\theta_2 \pm \theta_3)}\right] \tag{13}$$

The BER of $s_1(t)$ may be obtained after considering all the transmitting signal combinations.

$$P_1 = \frac{1}{2}\left(Q\left(\sqrt{r}\,|\cos(\theta_2 + \theta_3)|\right) + Q\left(\sqrt{r}\,|\cos(\theta_2 - \theta_3)|\right)\right) \tag{14}$$

Finally, if $s_1(t)$ and $s_2(t)$ are public signals, the BER of $s_3(t)$ can be expressed as (11). In the same way, if $s_1(t)$ and $s_3(t)$ are public signals, the BER of $s_2(t)$ can be expressed as (12).

IV. QUADRA-CHANNEL SIGNAL DEMODULATION THRESHOLD

In addition to these CEM methods above, multi-frequency multiplexing techniques, which can combine signals from separate sidebands, are required for some special cases, such as the E5 band for Galileo and the B2 band for Beidou Phase III. So far, many constant-envelope multiplexing methods for Quadra-channel signal demodulation have been proposed, such as Alternate BOC (AltBOC) [15], Time Division AltBOC (Td-AltBOC) [16], Dual-QPSK [17], bipolar subcarrier (BS-ACEBOC) [18] and Phase-Optimized constant-envelope Transmission (POCET) [19]. POCET yields a phase table which addresses the correspondence between the transmission phase and the values of the original signals through optimization, thus resulting in an optimal efficiency. It treats the constant-envelope multiplexed signal as a Phase Shift Keying (PSK) signal and transforms the constant-envelope multiplexing method into a phase-mapping problem. On the other hand, if the phases of the received signal are known, the transmitted signal code sequence can be recovered according to the phase table.

For a constant-envelope signal containing an N_0 signal component, there are 2^{N0} kinds of combinations, namely, a maximum of 2^{N0} phase states. Through the analysis above, it can be summarized that the best recovery bit error rate is no more than the Multiple Phase Shift Keying (MPSK) code error performance under Gaussian noise channels. The BER of MPSK can be written as [20]

$$P_e \approx e^{-r\cdot\sin^2(\pi/M)} \tag{15}$$

where the r (represents SNR) in the equation is high enough. M stands for the number of signals modulated.

In the actual satellite navigation system, it is usually required to transmit the OS signal and the AS signal together. The accurate tracking of the OS signal components is useful for the recovery of the AS signal components. For M signals that adopt POCET modulation, we only need to distinguish between the $2^{N_0-N_1}$ phase points if there are N_1 signal components known, which effectively improves the accuracy of the signal code sequence recovery.

V. DISCUSSION RESULTS AND ANALYSIS

The standard codes are generated according to the ICD at first. Then, the modulated signals are added through the Gaussian noise channel under different CNRs. The non-public codes are recovered by the method referred to in this paper. A series of Monte Carlo simulations is conducted to make the results close to the actual situation [21].

First, the effects of carrier phase tracking errors on the BERs is analysed. The received GNSS baseband signals can be expressed as

$$r(t) = s(t)\cos(2\pi f_d t) + n(t) \tag{16}$$

where $s(t) = \pm 1$ and f_d is the residual doppler. Then, the BER can be expressed as

$$P_{BER} = P\left(sign\left(r(t)\right) = s(t)\right) \tag{17}$$

If the time is long enough and the signal is strong enough, then the BER is approximately equal to 0.5. The BER curves in 1 ms can be obtained in a condition of SNR = 5 dB as shown in Fig. 5.

The effects of carrier phase tracking errors and noise on the BERs under SNR = 5 dB (blue line) is shown in Fig. 5, where the red line is only affected by noise. The figure shows that the BER increases with the increase of residual doppler. However, the actual residual doppler in a tracking loop is usually only a few Hertz. Therefore, it can be regarded as noise. Therefore, the following analysis only considers the influence of noise.

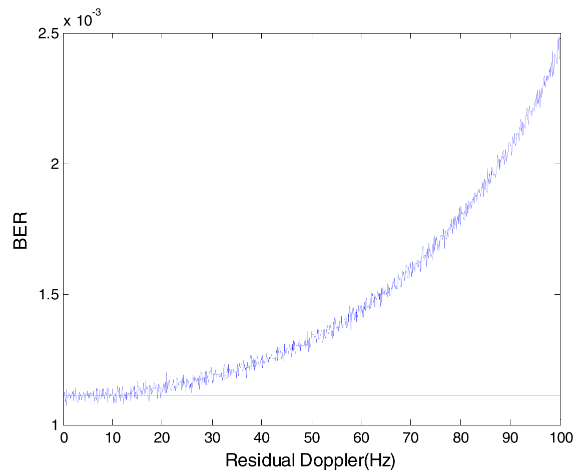

FIGURE 5. The effects of carrier phase tracking errors on the BERs under SNR = 5 dB.

A. TRI-CHANNEL SIGNAL MODULATION

The new restricted M-code service was introduced in the GPS block IIR-M SVs. The BOC(10,5) signal of that serviceis designed to be an overlay to the P(Y)-code signal in the I-channel. A CASM approach may be applied to form a constant envelope. The signal power level of the C/A code is normalized to 0 dBW, and then the P(Y) code and the M-code signal power are −3 dBW and 0 dBW, respectively. The carrier of the C/A code signal and P(Y) code shall be in the orthogonal phase. The bandwidth used in the simulation below is 1.023 MHz.

When the C/A code signals and the inter-modulation components are in the quadrature channel, whereas the P (Y) code signal and M-code signal are in the in-phase channel, a possible solution is $\theta_2 = 45^o$ or $\theta_3 = 215.3^o$. Then, the recovery P(Y) and M-code BER can be obtained according to the scatterplot.

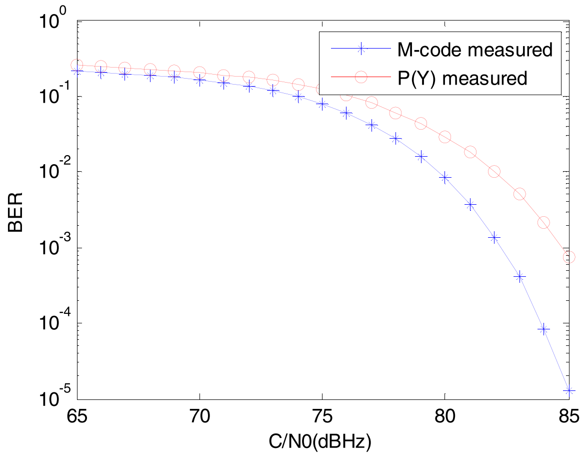

FIGURE 6. P(Y) and M-code BER when C/A code is in Q channel under different CNRs.

Fig. 6 shows that the measured P(Y) and M-code BER do not reach the 10^{-3} BER performance level until the C/N_0 is greater than 85 dBHz. This is nearly impossible for a received navigation signal. Because the received minimum RF signal strength for Block II-M satellites in a 20.16 MHz bandwidth on L1 is −161.5 dBW.

However, this is at the beginning of the modernization of GPS signal design. There are three combinations according to the relationship among C/A, P(Y), and M-code. It may have similar results as the C/A code located in the in-phase channel. As the C/A code is modulated in the in-phase channel, such as the $s_2(t)$ in (4), the M-code is $s_3(t)$ and the P(Y) code is $s_1(t)$ in (4), a possible solution is $\theta_2 = 54.7^o$ or $\theta_3 = 234.7^o$. Then, the P(Y) and M-code can be recovered after tracking the C/A code. By comparison with the original code sequence, BER curves can be obtained as shown in Fig. 7.

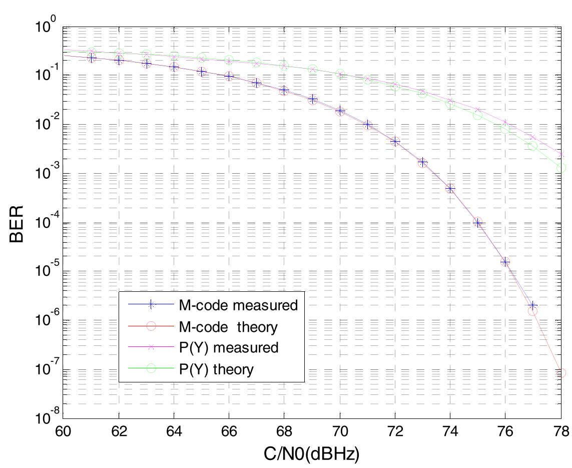

FIGURE 7. P(Y) and M-code BER when C/A code is in I channel under different CNRs.

The M-code BER consistent with the theoretical bit error rate is shown in Fig. 7. We can get a 10^{-3} BER performance once the C/N0 is greater than 73 dBHz. However, the P(Y) code orthogonal to the C/A code does not reach the 10^{-3} BER performance until the C/N0 is greater than 80 dBHz.

It can also be seen from Fig. 6 and Fig. 7 that the current constant-envelope modulation plan in Fig.6 is safer than the plan in Fig. 7. The former requires a higher SNR to recover the AS signal component for both the P(Y) code and the M-code.

B. QUADA-CHANNEL SIGNAL MODULATION

GPS III will broadcast the new $L1C_D$ and $L1C_P$ signal components in L1 combined with the C/A and P(Y) code signals. We assume the four signals will be transmitted in a constant-envelope modulation, whereas the M-code signal will be transmitted in another channel after it is power enhanced. Carriers of the two L1C components shall be in the same phase as the P(Y) code carrier. The baseband signal of L1 can be expressed as

$$\begin{aligned} s_{L1}(t) &= Ae^{j\theta(t)} \\ &= A_1\left(S_{C/A}(t) + j\alpha S_{P(Y)}(t) + j\beta S_{L1C_P}(t)\right. \\ &\quad \left. + j\gamma S_{L1C_D}(t)\right) + e(t) \end{aligned} \tag{18}$$

where A_1 is the amplitude of the C/A code signal, the coefficient $\alpha = 0.7071$, $\beta = 1.0288$, $\gamma = 0.5957$, and $e(t)$ represents cross-product (intermodulation) terms. $\theta(t)$ varies among the 16 phase points in the POCET modulated signal.

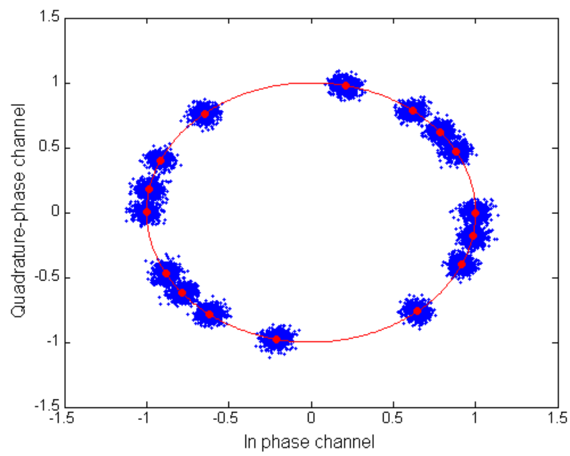

FIGURE 8. Scatterplot for a POCET modulated combination of C/A, P(Y), $L1C_P$, and $L1C_D$ signals under the SNR of 25 dB.

The scatterplot of the L1 signal using a POCET modulation under 25 dB is shown in Fig. 8, where the red dots indicate ideal constellation points and blue scatter for actual constellation points. It can be seen that certain confusion has occurred under the condition of 25 dB. As the received satellite signals can hardly reach such a high SNR, it is almost impossible to recover chip symbols by differentiating signal components through constellation points.

However, the C/A code, $L1C_D$ code and $L1C_P$ code signal components are all civil code signal components, whose chip symbol can be obtained through the carrier wipe-off and pseudo code tracking. The polarity of the P(Y) code signal component can be determined between two of 16 phase points.

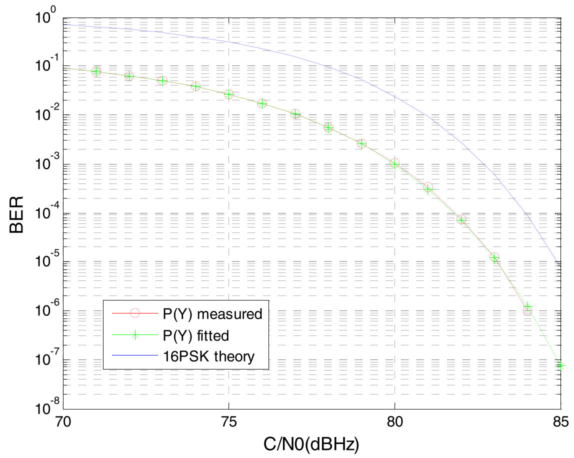

FIGURE 9. P(Y) Bit error Rate for a POCET modulated combination of C/A, P(Y), L1Cp, and L1Cd code signals.

Fig. 9 shows the bit error rate of the P(Y) code signal component under a POCET modulation. The P(Y) code signal is obtained by the minimum distance criterion. We build a fitting model through a Q-function. The red lines represent the measured bit error rate of the P(Y) code, and the green line represents the fitted values. The fitting expression is

$$P_1 = 0.5 \cdot Q\left(0.2 \cdot \sqrt{r}\right) \tag{19}$$

The figure shows that the recovered P(Y) bit error rate should be less than 10^{-3}, if the SNR is greater than 80 dBHz, which means the receiving antenna dish diameter is larger than 13 m without considering transmission cable.

VI. CONCLUSION

The satellite navigation system with limited onboard power widely adopts a constant-envelope design to transmit signals. AS signals and OS signals are often transmitted through a unified constant-envelope. It offers the possibility for the demodulation of the PN code sequence in the AS signal.

This paper established models of signal components under different constant-envelope demodulations. It analysed the demodulation threshold of the AS signal under the requirement of BER $= 10^{-3}$. When dual-channel signals use QPSK demodulation, the AS signal components recovery performance is similar to the BER of BPSK. It can realize a BER of 10^{-3} until the C/N_0 exceed 70 dBHz. When using a CASM/Interplex multiplexing mode on the tri-channel signal, at least one signal component should be known, and only the AS signal and the OS signal that are in the same branch can be recovered. The demodulation threshold may be lower than 73 dBHz. If they are located on the orthogonal branch, the OS signals play a negligible role in the AS signals to be recovered. When using POCET multiplexing mode on the quadra-channel signal, the demodulation threshold needs to be higher than 80 dBHz under the condition that one-channel signal is unknown.

This paper puts forward an idea for the recovery of navigation AS signal components and reports the demodulation threshold of the AS signal under different constant envelope modulations. It also provides a reference for the analysis, evaluation and system optimization design of a GNSS signal.

ACKNOWLEDGMENT

The authors would like to thank Dr. Kou Yanhong for providing the scattering model of airplane. They also wish to thank all the anonymous reviewers and editors for their helpful comments and suggestions for the improvement of this paper.

REFERENCES

[1] G. X. Gao, "Towards navigation based On 120 satellites: Analyzing the new signals," Dept. Electr. Eng., Stanford Univ., Stanford, CA, USA, 2008, pp. 31–37.

[2] H. Chengyan, "Research on evaluation methods of GNSS signal quality and the influence of GNSS signal on ranging performance," Nat. Time Service Center, Chin. Academy Sci., Beijing, China, 2013, pp. 158–161.

[3] C. J. Hegarty, "GNSS signals—An overview," in *Proc. IEEE Int. Freq. Control Symp. (FCS)*, May 2013, pp. 1–7.

[4] *Anon, Navstar GPS Space Segnent/Navigation User Interfaces Specification (IS-GPS-200H)[S]*, Sep. 2013

[5] H. Li and M. Lu, "Research on global positioning system M-code acquisition method and the acquisition performance," *IET Commun.*, vol. 8, no. 5, pp. 587–596, 2014.

[6] *Anon, Global Positioning Systems Directorate Systems Engineering & Integration Interface Specification, (IS-GPS-800D)*. United States Coast Guard, Washington, DC, USA, Sep. 2013.

[7] J. M. Parro-Jiménez, J. A. López-Salcedo, R. T. Ioannides, and M. Crisci, "Frequency-domain code replica detection for a GNSS receiver," in *Proc. Int. Conf. Localization GNSS (ICL-GNSS)*, Jun. 2013, pp. 1–6.

[8] W. Xiao, L. WX, and S. GF, "Modernization milestone: BeiDou M2-S initial signal analysis," *GPS Solutions*, vol. 20, no. 1, pp. 125–133, 2016.

[9] G. W. Hein *et al.*, "MBOC: The new optimized spreading modulation recommended for GALILEO L1 OS and GPS L1C," in *Proc. Position, Location, Navigat. Symp. (IEEE/ION)*, San Diego, CA, USA, Apr. 2006, pp. 883–892.

[10] R. S. Orr, "Code multiplexing via majority logic for GPS modernization," in *Proc. 11th Int. Tech. Meeting Satellite Division Inst. Navigat.*, 1998, pp. 265–273.

[11] X. Zhang *et al.*, "Initial assessment of the COMPASS/BeiDou-3: New-generation navigation signals," *J. Geodesy*, vol. 91, no. 10, pp. 1125–1240, 2017.

[12] G. H. Wang, V. S. Lin, T. Fan, K. P. Maine, P. A. Dafesh, and B. Myers, "Study of signal combining methodologies for GPS III: Flexible navigation payload," in *Proc. 17th Int. Tech. Meeting Satellite Division Inst. Navigat.*, Long Beach, CA, USA, 2004, pp. 2207–2218.

[13] S. Butman and U. Timor, "Interplex—An efficient multichannel PSK/PM telemetry system," *IEEE Trans Commun*, vol. TC-20, no. 3, pp. 415–419, Jun. 1972.

[14] P. A. Dafesh, "Coherent adaptive subcarrier modulation (CASM) for GPS modernization," in *Proc. 12th Nat. Techn. Meeting Inst. Navigat.*, San Diego, CA, USA, 1999, pp. 649–660.

[15] L. Lestarquit, G. Artaud, and J. Issler, "AltBOC for dummies or everything you always wanted to know about AltBOC," in *Proc. ION GNSS Inst. Navigat.*, Savannah, CA, USA, 2008, pp. 961–970.

[16] Z. Tang *et al.*, "TD-AltBOC: A new COMPASS B2 modulation," *Sci. China Phys., Mech. Astron.*, vol. 54, pp. 1014–1021, Jun. 2011.

[17] K. Zhang, H. Zhou, and F. Wang, "Multiplexing performance assessment of POCET method for compass B1/B3 signals," *J. Navigat.*, vol. 64, no. 1s, pp. S41–S54, 2011.

[18] F. Guo, Z. Yao, and M. Lu, "BS-ACEBOC: A generalized low-complexity dual-frequency constant-envelope multiplexing modulation for GNSS," *GPS Solut.*, vol. 21, no. 2, pp. 561–575, 2016.

[19] P. A. Dafesh and C.R. Cahn, "Phase-optimized constant-envelope transmission (POCET) modulation method for GNSS signals," in *Proc. 22nd Int. Techn. Meeting Satellite Division Inst. Navigat.*, Savannah, GA, USA, 2009, pp. 2860–2866.
[20] J. A. A. Rodríguez, "On generalized signal waveforms for satellite navigation," Faculty Aerosp. Eng., Univ. FAF Munich, Munich, Germany, 2008.
[21] C. Cho, J.-G. Lee, J.-H. Kim, and D.-C. Kim, "Uncertainty analysis in EVM measurement using a Monte–Carlo simulation," *IEEE Trans. Instrum. Meas.*, vol. 64, no. 6, pp. 1413–1418, Jun. 2015.

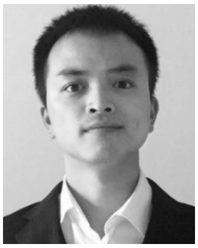

WEI XIAO was born in Pingxiang, China, in 1992. He received the B.S. degree from Beihang University in2012 and the M.S. degree from the National University of Defense Technology in 2014, where he is currently pursuing the Ph.D. degree in information and communication engineering. His current interests include GNSS signal analysis and GNSS integrity (RAIM, WAAS, and SAIM), and GNSS receiver positioning algorithm.

WENXIANG LIU was born in Yichun, China, in 1981. He is currently a Lecturer with the College of Electronic Science and Engineering, National University of Defense Technology, Changsha, China. He has been actively involved in many aspects of GNSS since 2005, including GNSS data processing, GNSS integrity monitoring (RAIM and SAIM), and GNSS receiver positioning algorithm. He has authored of over 30 papers and the co-inventor of two patents. He has been leading over four national research projects' work since 2012.

WEIHUA MOU was born in Jiaozhou, China, in 1979. He is currently pursuing the Ph.D. degree with the National University of Defense Technology. He is also an Associate Professor with the College of Electronic Science, National University of Defense Technology. His main research interests include GPU parallel computing, GNSS signal simulation, and receiver development.

LING YONG was born in Chongqing, China, in 1973. She is currently an Associate Professor with the College of Electronic Science and Engineering, National University of Defense Technology, Changsha, China, where she is also a Professor of a number of courses related to satellite navigation, and get a high evaluation. She has been actively involved in many aspects of GNSS since 1999, including GNSS signal processing, GNSS signal simulating, and GNSS receiver designing. She has authored of over 15 papers, and has been leading over five national research projects since 1999.

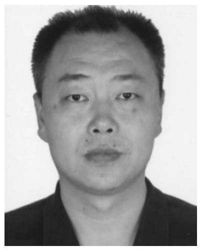

GUANGFU SUN was born in Ha Erbing, China, in 1970. He received the M.S. and Ph.D. degrees from the College of Electronic Science, National University of Defense Technology, Changsha, China. He is currently a Professor with the College of Electronic Science and Engineering, National University of Defense Technology. He is responsible for research and teaching in the field of algorithm designs and the performance analyses of global navigation satellite systems, application-specified integrated circuit, and communication.